View Article Online
View Journal

Dalton Transactions

An international journal of inorganic chemistry

Accepted Manuscript

This article can be cited before page numbers have been issued, to do this please use: A. Pinto, G. Spigolon, R. Gavara, C. Zonta, G. Licini and L. Rodriguez, *Dalton Trans.*, 2020, DOI: 10.1039/D0DT02564J.

ROYAL SOCIETY OF CHEMISTRY

rsc.li/dalton

Tripodal gold(I) polypyridyl complexes and their Cu^{+} and Zn^{2+} heterometallic derivatives. Effects on luminescence

Andrea Pinto,[a,b] Giulia Spigolon,[c] Raquel Gavara,[a] Cristiano Zonta,[c] Giulia Licini,[c,*] Laura Rodríguez[a,b,*]

[a] *Departament de Química Inorgànica i Orgànica, Secció de Química Inorgànica, Universitat de Barcelona, Martí i Franquès 1-11, E-08028 Barcelona, Spain. e-mail: laura.rodriguez@qi.ub.es*

[b] *Institut de Nanociència i Nanotecnologia (IN^{2}UB). Universitat de Barcelona, 08028 Barcelona, Spain*

[c] *Dipartimento di Scienze Chimiche and CIRCC – Unità di Padova, Università degli Studi di Padova, via Marzolo 1, 35131 Padova, Italy. e-mail: giulia.licini@unipd.it*

Abstract

The synthesis of three gold(I) tripodal complexes containing the tris(2-pyridylmethyl)amine (TPA) ligand coordinated to Au-PR_3 moieties (PR_3 = 1,3,5-triaza-7-phosphatricyclo[3.3.1.13.7]decane, PTA (**1**), 3,7-diacetyl-1,3,7-triaza-5-phosphabicyclo[3.3.1]nonane, DAPTA (**2**) and triphenylphosphane (**3**) was performed together with a cage-like structure containing the triphosphane 1,1,1-tris(diphenylphosphinomethyl)ethane (**4**). The luminescence of these complexes has been studied and they show a red shift upon formation of heterometallic complexes by reaction with $Zn(NO_3)_2$, CuCl and $[Cu(CH_3CN)_4]BF_4$. The different coordination motifs of the Zn^{2+} and Cu^{+} heterometallic species and the resulting changes on the recorded absorption, emission and NMR spectra were analysed and supported by TD-DFT calculations.

Keywords: gold(I), heterometallic complexes, luminescence, optoelectronics, TD-DFT

DOI: 10.1039/D0DT02564J

Introduction

Tris(2-pyridylmethyl)amine (TPA) which possesses four nitrogen atoms able for the ligation of a wide variety of metal ions, and its derivatives are a family of versatile ligands that has been extensively studied.[1] The mobility of its pyridine arms allows TPA to accommodate metal centers with different coordination geometries and electronic structures[2] with a wide variety of different application including optoelectronics, sensing[3–6] or catalysis[7,8] among others. The additional introduction of terminal alkynyl moieties allows the coordination with d^{10} coinage-metals, such as gold(I),[9] that are very well known to favor the coordination by the establishment of metallophilic contacts. Moreover, gold(I) complexes are an important class of complexes well known to facilitate a triplet excited state emission[10] and the formation of weak Au···Au interactions arising from relativistic effects, play a key role in the observed emission.[11] Additionally, the ability of the alkynes to bind late-transition metal ions in a bidentate mode through a combination of σ and π bonding has been extensively utilized in the synthetic chemistry of Cu, Ag, and Au. This coordination mode of alkynyl ligand provides additional opportunities for fine tuning of the photophysical characteristics of the resulting compounds.[12,13] This fact, together with the tripodal shape of the TPA ligand makes the resulting complexes particularly interesting due to their luminescent properties able to be modulated by the presence or absence of aurophilic contacts. The coordination of a second metal atom can play an important role in this process. However, controlling the formation of heterometallic arrays is more challenging in comparison with the formation of homometallic gold(I) species.

The second coordination position of the linear Au(I) complexes is frequently occupied by tertiary phosphanes, as ancillary soft donors. In general, they have less influence on the arrangement of the metal core and, consequently, on the photophysical properties of the complexes. Nevertheless, they have a particular influence on the solubility of the resulting complexes.[10,14–18]

The presence of several metal ions or atoms in one molecular entity often brings a cooperative effect and leads to the emergence of particular physical and chemical properties, which cannot be attributed to the sum of the properties of the monometallic components. Such synergistic functionality has significantly driven the experimental and

View Article Online
DOI: 10.1039/D0DT02564J

theoretical efforts that have impressively advanced the fundamental chemistry of polymetallic structures.[19]

Taking all of this into consideration, we have designed and synthesized different tripodal gold(I) alkynyl complexes derived from novel TPA ligands and containing three different monophosphanes and a triphosphane. The free coordinative positions of the pyridyl moieties of TPA have been explored in order to obtain Au(I)/Cu(I) or Au(I)/Zn(II) heterometallic structures with tunable photophysical properties.

Results and Discussion

Synthesis and Characterization

*Synthesis of tris-pyridyl alkynyl ligand, **L**.*

The synthesis of the tripodal complexes required the previous design and synthesis of the tripyrdidylmethylamine ligand **L**, containing three alkynyl moieties in *ortho* position with respect to pyridyl nitrogen as it is displayed in Scheme 1.

It is synthesized through the previous synthesis of **L1** and **L2** precursors via reductive amination of commercially available 6-bromo-2-pyridinecarboxaldehyde (**A**) with sodium borohydride triacetate and ammonium acetate (**L1**)[20] and the following three-fold Sonogashira coupling between **L1** and dimethyl ethynyl carbinol and deprotection with sodium hydroxide gaining the desired *tris*-pyridyl ethynyl ligand **L** in 60% yield. The correct formation of the product was confirmed by ^{1}H and ^{13}C NMR, IR and ESI-MS analysis (see SI). The presence of the terminal alkynyl proton was evidenced by the presence of the characteristic singlet at 3.18 ppm in the ^{1}H NMR spectrum (Figure S5) and the broad IR peak at 3278 cm^{-1}. ESI/MS spectrometry allowed the detection of the $[M+H^{+}]$ molecular peak (m/z = 363.2).

View Article Online
DOI: 10.1039/D0DT02564J

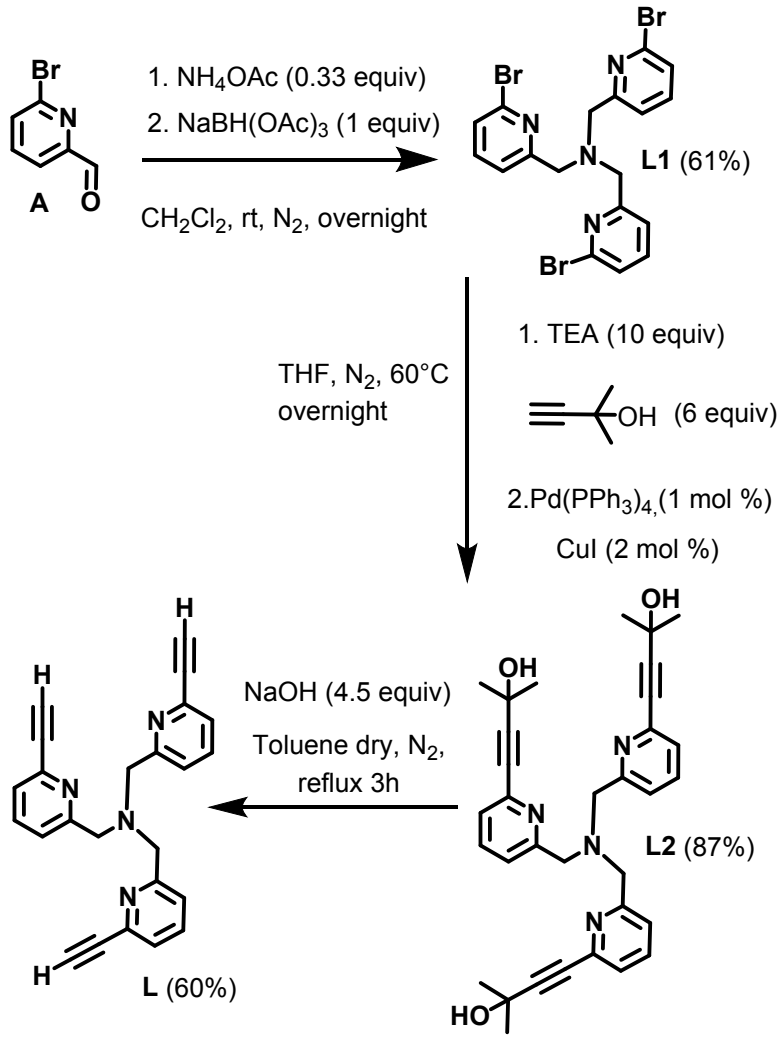

Scheme 1. Synthesis of ligand **L**.

Synthesis of tripodal gold(I) complexes.

$Au_3(PTA)_3L$ (**1**) and $Au_3(DAPTA)_3L$ (**2**) complexes were obtained by deprotonation of the terminal protons of the alkynyl groups in **L** and subsequent reaction with the previously synthesized $[AuCl(PR_3)]$ (PR_3 = PTA, DAPTA) precursors in 1:3 stoichiometry (see Scheme 2).

View Article Online
DOI: 10.1039/D0DT02564J

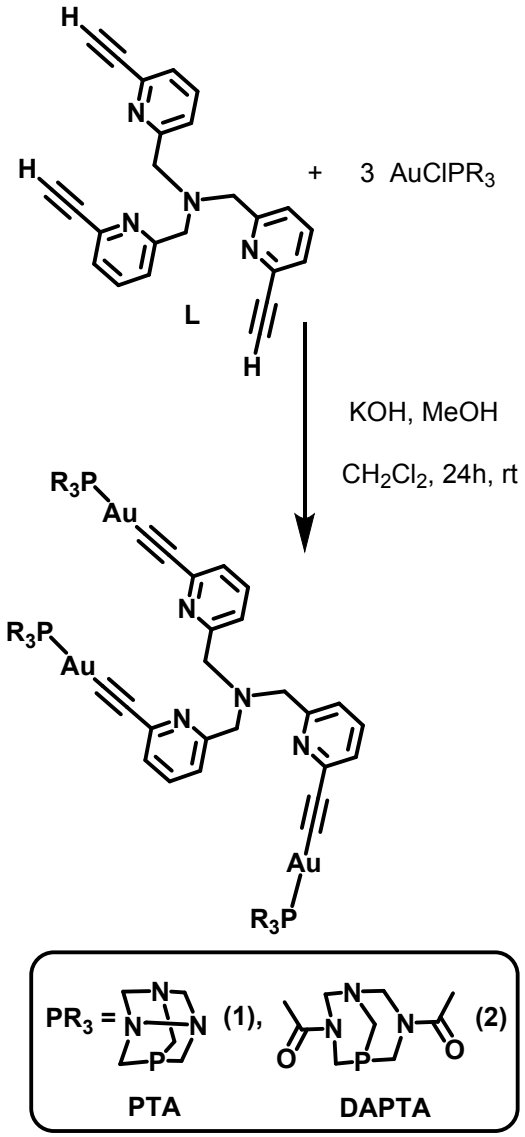

Scheme 2. Synthesis of complexes **1** and **2**.

This synthetic procedure was not successful in the case of the -$AuPPh_3$ derivative, **3**. In this case, the reaction could be performed by the previous substitution of the chloride ligand by the acetylacetonate (formation of the [$Au(acac)PPh_3$] complex) that reacts with the terminal protons of the tripodal ligand producing the coordination of the gold metal atom to the alkynyl moiety and acetylacetone as volatile by-product (Scheme 3).

View Article Online
DOI: 10.1039/D0DT02564J

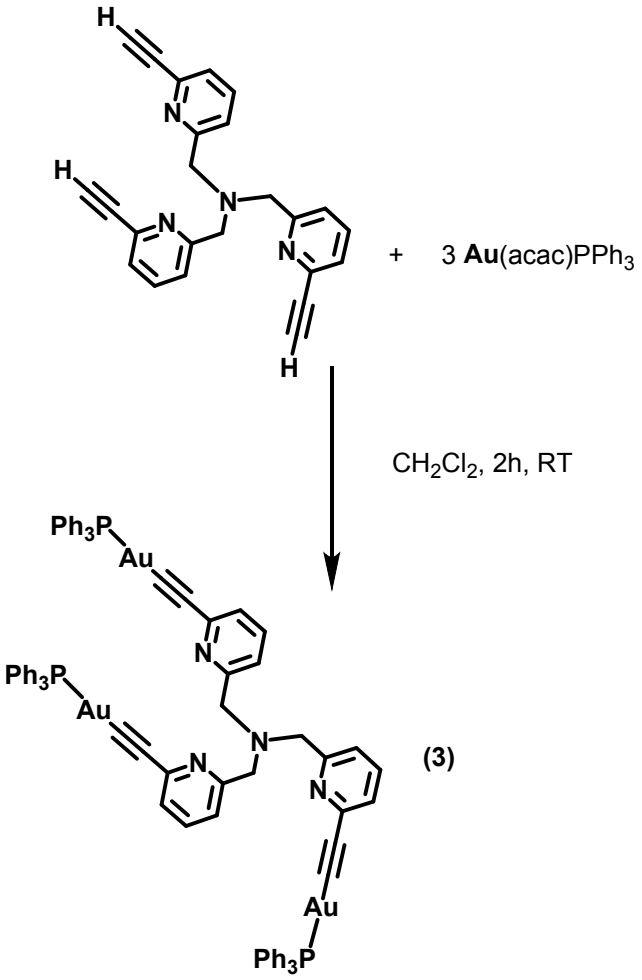

Scheme 3. Synthesis of complex **3**.

All complexes were obtained as a yellow solid stable to air and moisture. Their spectroscopic data are in accordance with the proposed stoichiometry. ^{1}H NMR spectra display the typical pattern of the phosphanes, the protons of the pyridine moiety and the disappearance of the terminal alkynyl protons upon formation of the complexes. ^{31}P{^{1}H} NMR shows only one signal at *ca.* -52 ppm (**1**), 3 ppm (**2**) and 29 ppm for (**3**), which confirms the equivalence of the phosphorous atoms in the molecules and their coordination to the gold centers (Figures S7-S12). The difference in the phosphorus-31 chemical shifts observed in **1** and **2** is significant but similar to analogues compound reported in the literature.[17a] This can be due to the different bond angle and stereoelectronic effects of both TPA and DAPTA phosphanes giving rise to different chemical shift anisotropy and the observed different phosphorus-31 chemical shift.[17b]

IR spectra show signals corresponding to the C≡C vibration at *ca.* 2100 cm^{-1} together with the disappearance of the signal of the terminal C≡C-*H* proton, the CH_2-P vibrations of the phosphanes and the C=O strong band in the case of **2**. Final evidence of the formation of the complex was given by ESI-MS: *m/z* 1422.274 for **1**, Figure S9 ([M + H^+]), 557.098 ([M+3H^+ + MeOH]) for **2** and 1737.300 ([M + H^+]) in the case of **3**.

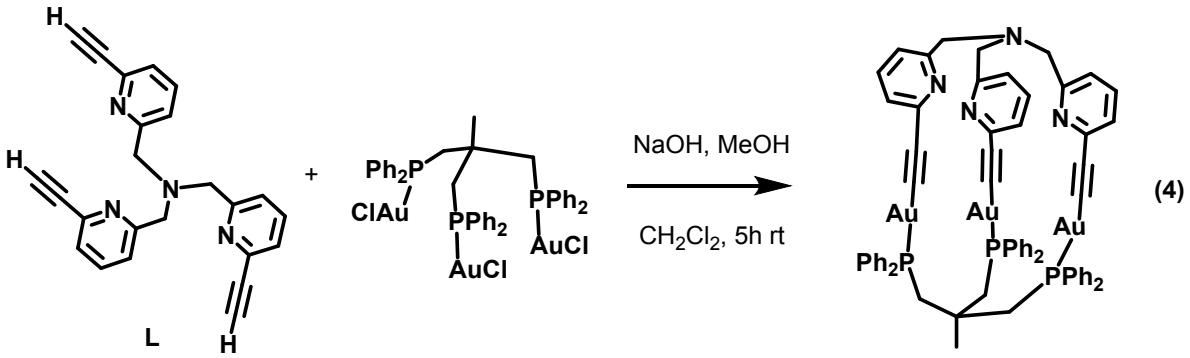

(4)

Scheme 4. Synthesis of cage complex **4**.

The reaction of **L** with (triphos)$(AuCl)_3$ (triphos = 1,1,1-tris(diphenylphosphinomethyl)ethane) in 1:1 ratio was also assayed in order to obtain a cage complex following the same conditions previously detailed for **1** and **2** (Scheme 4). The correct formation of the cage-like compound **4** was evidenced by ESI-MS [molecular peak at *m/z* 1592.290 ([M+NH_4^+])], expected bands in the FT-IR (C≡C, C=N, C=C and PPh_2 vibrations, Figure S14) and ^{1}H and ^{31}P NMR spectra, although in this case, the solubility of the complex is considerably lower (Figures S15-S16).

Photophysical characterization

Absorption and emission spectra of all complexes were recorded in DMSO and acetonitrile at 10^{-5} M concentration and the results are summarized in Table 1. The absorption spectra of the gold(I) complexes recorded in DMSO display vibronically resolved broad bands centered at *ca*. 300 nm (Figure 1). The pattern is similar to the previously reported for other alkynyl pyridyl derivatives and it may be thus ascribed to intraligand [$\pi \rightarrow \pi^*$ (C≡C or C≡C-py)] character.[2,16,21–25]

View Article Online
DOI: 10.1039/D0DT02564J

Compound	Absorption λ_{max} (nm) (ε (10^3 M^{-1} cm^{-1}))	Emission λ_{max} (nm) DMSO	Emission λ_{max} (nm) acetonitrile	Emission, λ_{max} (nm) solid
L	283 (5.2)	440	400	-
1	268 (2.9), 306 (42.4)	472[a]	529	531
2	275 (29.7), 305 (31.2)	473[a]	525	530
3	300 (22.3)	441 [a]	481	-
4	278 (15.4)	440[a]	-	-

Table 1. Absorption and emission data of homometallic gold(I) complexes **1-4** and ligand precursor, L. λ_{exc} = 350 nm. [a] Low intensity bands.

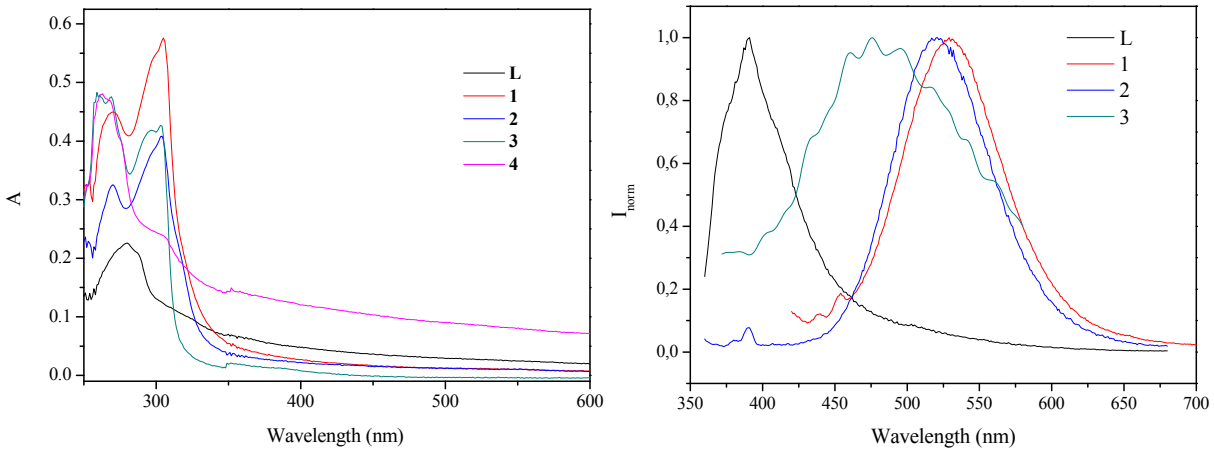

Figure 1. Absorption spectra in DMSO (left) and normalized emission in acetonitrile (right) of compounds **L** and **1-4** at *ca*. $1 \cdot 10^{-5}$ M.

An increase on the baseline in the absorption spectra can be also detected in the case of **4**, which results from scattering effects due to the presence of small aggregates[15] in agreement with the lower observed solubility of the cage-like complex in this solvent. The same scattering is observed in all cases when the spectra are recorded in acetonitrile (Figure S17), where samples are not perfectly dissolved. In order to provide further

View Article Online
DOI: 10.1039/D0DT02564J

evidences of these aggregates, UV-vis absorption spectra at different DMSO-water contents mixtures were examined (Figure S18). The absorption bands at *ca*. 300 nm become broader when the water content is increased, and the shoulder at *ca*. 350 nm becomes the main band together with a clear increase of the baseline. All these profiles are in agreement with aggregates' formation.[15]

Excitation of the samples at 350 nm in DMSO solutions displays only significant emission in the case of **L** and the emission is very weak in the presence of gold, probably due to non-radiative decays from a previously populated triplet state due to the heavy atom effect of the gold atom. On the other hand, the aggregated samples display intense emission centered at *ca*. 530 nm both in DMSO/water mixtures (Figure S18) and in acetonitrile (Figure 1) in the case of the three open tripodal complexes **1**-**3** (~530 nm for **1** and **2** and ~480 nm in the case of **3**). No significant emission was recorded for cage-like complex **4**. The broad shape of the emission band indicates an excimeric emission in all cases. The open conformation of the tripodal complexes can easily favor the contact between the different branches of the molecules in solution, being supported by the establishment of different type of weak contacts, such as Au(I)···Au(I) bonds or π–π interactions (in agreement with intra- and/or intermolecular aggregates). Thus, the emission has being assigned to triplet metal-perturbed intraligand π-π*(C≡C) transitions or ^{3}MMLCT transitions according to literature.[10,18,21,25–29] The large Stokes shift and the increased emission intensity upon deoxygenation of the samples support the phosphorescence assignment. In solid state significant emission could be recorded only for **1** and **2,** with emission maxima that fits perfectly with the recorded for aggregated samples in solution (Figure S19).

Tuning luminescence by the formation of heterometallic complexes.

One way to modulate the luminescence properties of the complexes is the formation of heterometallic structures, which will introduce changes on the three-dimensional conformation of the molecules upon coordination with a second metal and to the additional intrinsic transitions resulting from the new complexes. We would like to exploit this methodology in our work by the reaction of **1**-**4** with Zn(II)- and Cu(I)- salts that have been chosen due to the well-known ability of these metals to coordinate amines (Zn(II) and Cu(I)) and alkynyl groups (in the case of Cu(I)), both present in **L**.[30–32]

Preliminary analyses of the possible formation of heterometallic complexes were performed by absorption and emission titrations that allowed us to identify the final stoichiometry of the resulting heterometallic structures as 1:1 (Figures 2 and S20-S28). In this way, absorption and emission spectra were recorded after addition of increasing amounts of Zn(II) and Cu(I) salts into a $1 \cdot 10^{-5}$ M solutions of complexes **1**-**3**. The very low solubility of **4** precluded to carry out this type of studies.

Interestingly, two different trends were observed, depending on the nature of the phosphanes. In the case of the more polar derivatives **1** and **2**, a progressive decrease on the absorption baseline is observed in all titration experiments, as an indication of disaggregation of the Au(I) complexes and formation of more soluble heterometallic complexes in this solvent. A decrease of the absorption band is observed in the presence of increasing amounts of Zn^{2+} while a blue shift is recorded in the presence of Cu^{+}- salts. This is indicative of different coordination modes of the resulting Zn^{2+} and Cu^{+} heterometallic complexes as well as a less favored electronic transition (higher energy transition) upon Cu(I) coordination. On the other hand, the addition of Zn(II) and Cu(I) salts into a solution of **3**, induces the formation of a lower energy band in all cases (Figures S26-S28) together with the presence of an isosbestic point at *ca*. 310 nm in the case of the Zn(II)/Au(I) heterometallic derivative (Figure S24). These changes are in agreement with modifications in the chemical structure involving the *tris*-amine part of the molecule.[1,30]

A progressive quenching of the emission band is observed in all cases, which is more significant in the case of Cu(I) salts, supporting a stronger interaction with this metal (Figure 2). The analysis of the observed spectral variations prompted us to calculate the association constants using the HypSpec 1.1.33 software for Windows [33] and revealed a different behaviour for the heterometallic complexes involving Au(I)/Zn(II) and Au(I)/Cu(I). In the first case, the data fit well to a complex with 1:1 stoichiometry (see Figure S19 for analysis of formation of **1a**). In the case of Au(I)/Cu(I) systems the formation of the 1:1 complex did not provide good fittings and it was necessary to take into account the formation of intermediate species with a 2:1 stoichiometry (two molecules of gold(I) complex per 1 molecules of Cu(I) salt) to obtain good results. This latter species would be favoured at lower concentrations of copper salt, while further addition of copper salt would shift the equilibria to the most stable 1:1 complex, as

supported by the higher equilibrium constants calculated for the 1:1 complex (see Table 2 and Figures S21-S22 for analysis of the titrations involving **1** and Cu(I) salts).

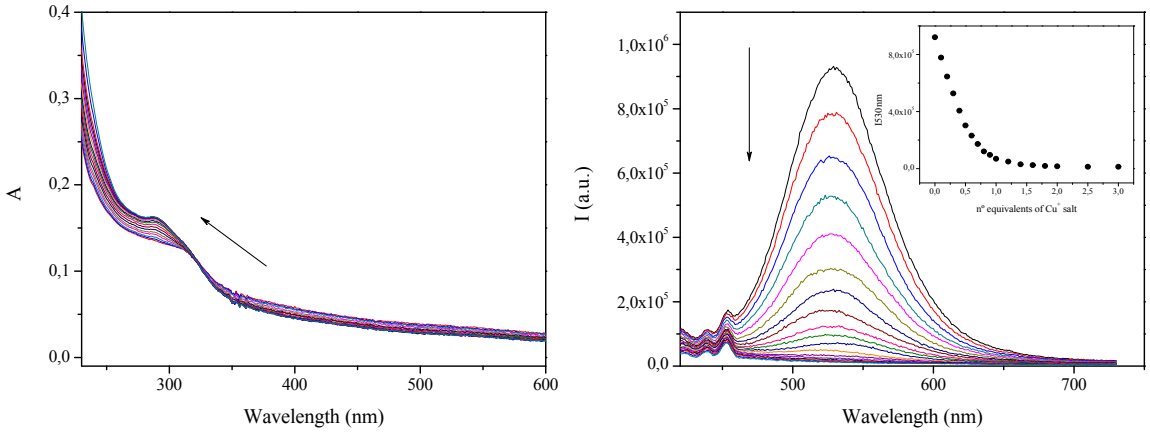

Figure 2. Absorption (left) and emission (right, λ_{exc} = 350nm) titrations of **1** with increasing amounts of CuCl. Inset: Plot of the variation of emission maximum against number of equivalents of Cu(I) salt.

Table 2. Association constant values calculated for the heterometallic complexes from the fitting of the emission titrations. In the table A refers to the homometallic gold(I) complex and B to the corresponding Zn(II) or Cu(I) salt.

Heterometallic complex	**log*K*(AB)**	**log*K*(A_2B)**	**Logβ(A_2B)**
1a	5.166±0.002	-	-
1b	6.673±0.016	5.833±0.007	12.506±0.012
1c	6.560±0.014	5.188±0.008	11.748±0.010
2a	5.014±0.003	-	-
2b	6.718±0.014	5.316±0.007	12.035±0.011
2c	7.323±0.015	5.678±0.003	13.001±0.014
3a	5.613±0.046	-	-
3b	6.226±0.064	5.143±0.220	13.369±0.243
3c	6.176±0.034	5.498±0.061	11.674±0.078

The corresponding heterometallic Au(I)/Zn(II) and Au(I)/Cu(I) complexes were then synthesized and isolated as orange or red powders by the direct addition of the Cu(I) (Cl^- and BF_4^-) or Zn(II) (NO_3^-) salts to independent solutions of the gold complexes (Scheme 5). Stoichiometric conditions were used for copper derivatives while an excess of Zn(II) was required for the isolation of the corresponding complexes in pure form (see Experimental Section) in agreement with the different binding strength of the resulting heterometallic complexes. An alternative method was used in the case of the heterometallic derivatives from **4** (**4a-c**) due to the low solubility of this compound in common solvents and to the closed-structure of the complex that may hinder the interaction with the corresponding cation once the cage is formed. The reaction was then performed in a one-pot synthesis by the addition of the corresponding Cu(I) and Zn(II) salts in the same reaction mixture containing the precursors for the synthesis of **4** (Scheme S1).

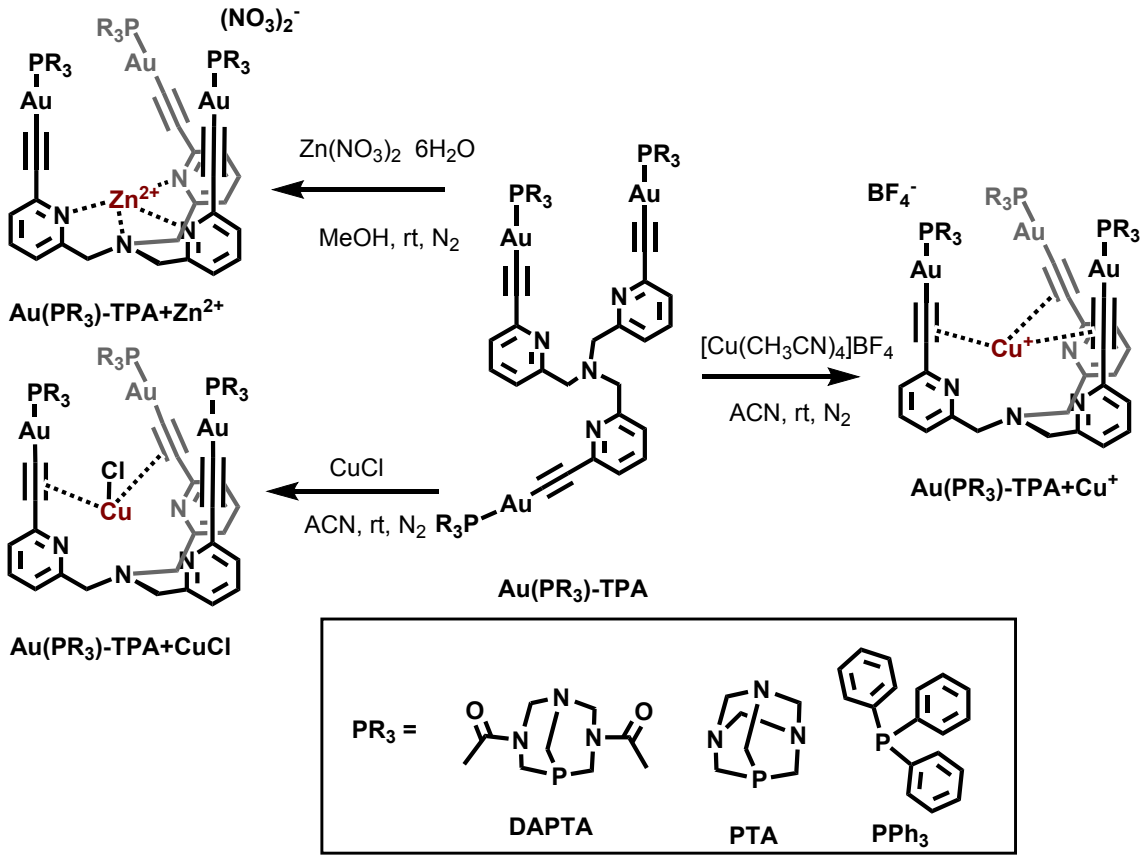

Scheme 5. Synthesis of Zn^{2+}- and Cu^{+}- heterometallic complexes obtained from **1**-**3**.

^{1}H NMR spectra evidences the different coordination motifs for Zn(II) and Cu(I) complexes (Figures 3 and SI). The methylene protons in the TPA moiety appear in the ^{1}H NMR spectra of Zn(II)-complexes broader than their homometallic precursors. Different shifts are observed for the pyridyl protons, being upfield shifted for *a* protons (closer to the central methylene group) and downfield shifted for *b* and *c* protons, as previously observed for other Zn-TPA complexes reported in the literature.[1,34,35] On the other hand, the global downfield shift of all the pyridyl protons recorded for Cu(I)-heterometallic systems, indicates that copper coordination occurs in the vicinity and evidences the different coordination motifs in comparison with Zn(II)-derivatives (Figure 3).

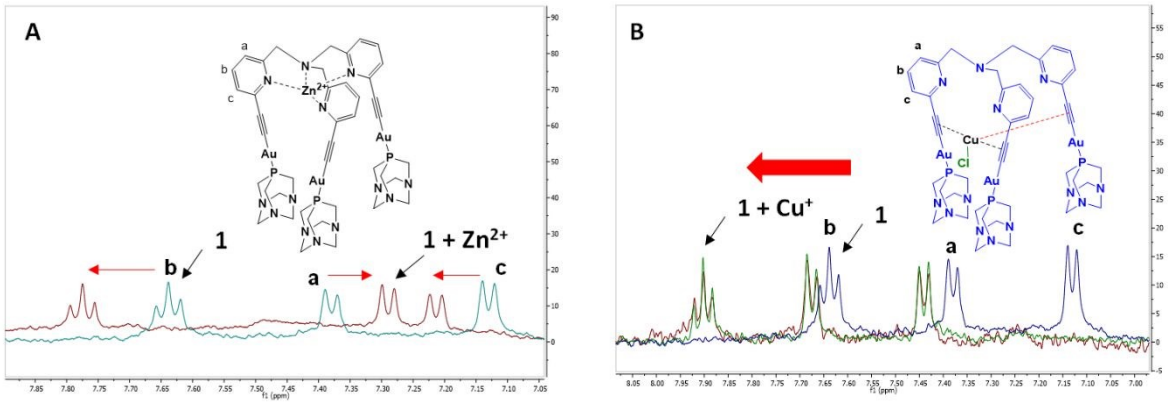

Figure 3. (**A**) ^{1}H NMR of compound **1** (green line) and with the addition of Zn^{2+} (brown line) and (**B**) ^{1}H NMR of compound **1** (blue line) and with the addition of CuCl and $Cu(CH_3CN)_4(BF_4)$ (green and brown line).

^{31}P NMR spectra display only one signal in all cases, as a direct proof of equivalent phosphorous atoms in solution (see SI). IR spectra suggest that the coordination of Cu(I) occurs through the alkynyl moiety, as reported in the literature,[36–39] since the stretching vibrations modes were affected with respect to the homometallic precursor. Nevertheless, the simultaneous coordination through N groups could not be excluded.[40–42] In addition, it was observed that a different coordination mode occurs depending on the two copper sources used in this work: CuCl or $[Cu(NCMe)_4]BF_4$. Two different stretching frequencies, one identical to homometallic gold(I) complex and another *ca*. 50 cm^{-1} shifted to shorter wavenumbers, were detected in the case of CuCl derivative, according to Cu(I)-coordination. However, two vibration bands (both shifted

to shorter wavenumbers) were obtained in the case of the reaction with $[Cu(NCMe)_4]BF_4$. The observed differences may be ascribed to the fact that chloride counterion is expected to be also coordinated to copper while BF_4^- is acting as external counterion and does not influence on the heterometallic species (Figure S54).[12,19,31] The mass spectra of compounds **xb** (x = **1**-**4**) confirms the presence of chloride in the structure and supports the different coordination of the two copper salts (Figure S33).

Significant differences can be also observed in the absorption spectra recorded for the different heterometallic complexes, that support the different coordination motifs. While the vibronic resolution is still maintained for Zn(II)-derivatives, Cu(I)-heterometallics display a complete broadening of the absorption pattern, in agreement with the decrease of the vibration modes of the alkynyl moieties blocked by coordination of Cu(I) (Figures S55-S58). The emission spectra of the solids are also an evidence of the correct formation of the zinc and copper heterometallic complexes. The large Stokes' shift is in agreement with phosphorescence emission with a metal-perturbed intraligand transition probably mixed with ^{3}MMLCT transitions, based on the literature.[9,18,25] It can be observed a gradual red shift in the emission wavelength in the order Au(I) complex - Au(I)/Zn(II) - Au(I)/CuCl – Au(I)/$Cu(BF_4)$ as shown in the Figure 4 and Table 3. It can be observed that the formation of the heterometallic cage-like derivatives **4a-c**, gives rise to an emission in solid state while **4** was not emissive (Figure S59).

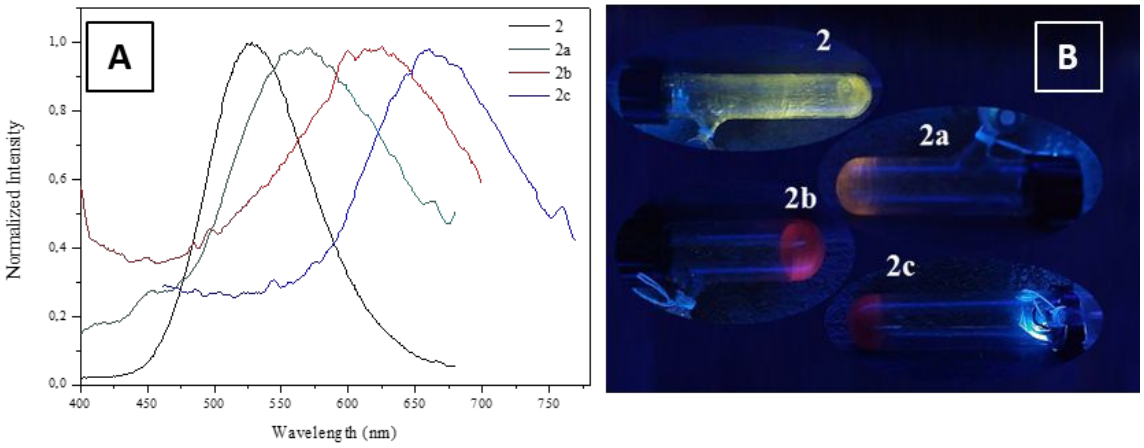

Figure 4. Normalized emission spectra in solid state of compounds **2**, **2a** (Au/Zn^{2+}), **2b** (Au(I)/CuCl) and **2c** (Au(I)/$Cu(BF_4)$) (left); image of the solids observed under UV light (right).

View Article Online
DOI: 10.1039/D0DT02564J

The observed changes in the emission are due to the different coordination motifs of the second metal ion and the change in the metallophilic interactions since, in the case of copper derivatives, Cu(I)···Au(I) interactions can take also place.[31,43] CuCl coordinates to the alkynyl moiety of two of the three units of the complex and the aurophilic/metallophilic interactions are more effective than for the respective gold homometallic complex. A global approximation of the three gold atoms is expected to be even stronger for the reaction with $[Cu(NCMe)_4]BF_4$, where Cu(I) coordinates to the three alkynyl moieties. On the other hand, coordination of the zinc cation is observed through the pyridyl moieties. Thus, the three arms of the tripodal unit become closer to each other for the copper heterometallic complexes and, in particular, for those having BF_4^- as external counterion. Although several attempts to grow single crystals suitable for X-ray diffraction failed, these statements are supported by the experimental data and comparison to literature.[12,31,43,44]

Table 3. Absorption data in DMSO and emission maximum (λ_{exc} = 350 nm) in solid state corresponding to the heterometallic gold(I) complexes **1-4a-c**.

Compound	Absorption λ_{max} (nm) (ε (10^3 M^{-1} cm^{-1}))	Emission, λ_{max} (nm) solid
1a	272 (40.0), 315 (41.7)	577
1b	288 (34.9)	600
1c	283 (34.9), 316 (32.4)	650
2a	273 (32.9), 306 (39.2)	571
2b	280 (23.7), 320 (20.9)	610
2c	284 (37.6), 317 (35.8)	662
3a	270(15.2), 311(2.1)	-
3b	270(16.0), 308(9.1)	-
3c	270(14.8),319(6.6)	-
4a	273 (38.2), 304 (38.0)	579
4b	273(38.1), 304(36.4)	626
4c	272(71.2), 305(63.7)	620

View Article Online
DOI: 10.1039/D0DT02564J

Theoretical Calculations

DFT (PBE0) calculations were performed for compound **1** and its heterometallic derivatives in order to support the coordination motifs of Zn(II) and Cu(I) in the homometallic complexes and the observed changes in their emission. As can be seen in Figure 5, the coordination of Zn(II) is expected to be produced through the nitrogen atoms of the TPA ligand. This allows the three gold atoms to get closer in space with a distance of 3.9 Å. The structure presents C_3 symmetry and the three gold atoms are the same distance. The Au(I)/Cu(I) heterometallic structures were also minimized considering the two expected situations (chloride coordination and Cu(I) coordination to two alkynyl moieties and BF_4^- free counterion with Cu(I) coordination to three alkynyl moieties). In the case of chloride coordination two gold arms get closer in the space and the chloride does not allow coordination of the third arm. In this situation all Au(I)···Au(I) distances are higher than 4 Å (6.4, 6.3 and 4.5 Å), but two short Cu(I)···Au(I) distances are observed. The removal of the chloride, as in the third structure without BF_4^-, induces a tighter metal assembly where four short metal-metal interactions are observed. In the latter case, all of the three Au atoms are interacting with copper and in addition a short Au(I)···Au(I) interaction is observed.The most important data is that intermetallic distances are expected to be in the order **1** > **1a** > **1b** > **1c**, in agreement with the recorded emission red-shift when going from the homometallic gold complex to the zinc and copper heterometallics.

View Article Online
DOI: 10.1039/D0DT02564J

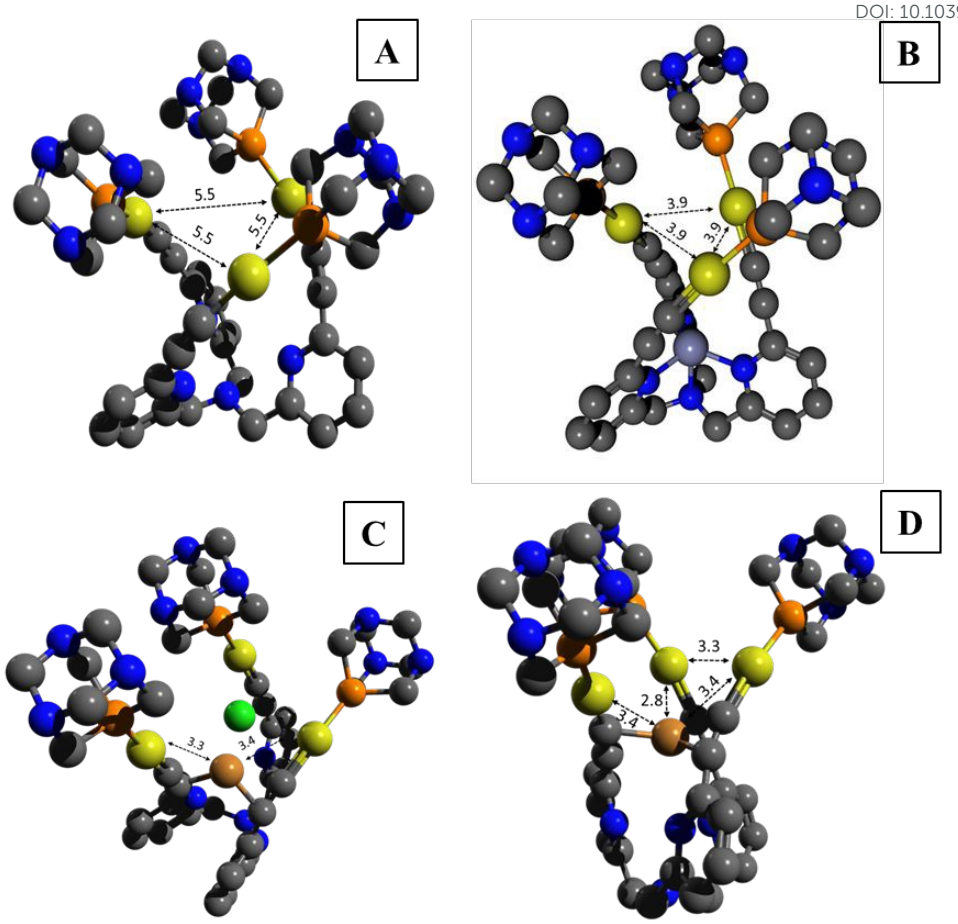

Figure 5. DFT structures for **1** (A), and the Zn-derivative, **1a** (B), with CuCl, **1b** (C) and $CuBF_4$, **1c** (D) derivatives. Intermetallic distances are indicated. Density functional theory (DFT) calculations were carried out by the use of the PBE0 functional. In the DFT energy calculations the def2-TZVPP basis set was used (including the def2-TZVPP pseudopotential for Au) and 6-31G(d,p) for all the other atoms.

Conclusions

The synthesis of four different gold(I) complexes with open (**1-3**) and cage-like structures (**4**) have been successfully accomplished following different experimental procedures depending on important parameters such as: i) solubility of the phosphane and resulting complex in organic and in polar media; ii) open or closed geometry.

The emission of the compounds in solution is more favoured in aggregated samples where Au(I)···Au(I) interactions must play a direct role in the resulting photophysical properties. Aggregation can be clearly detected by increase on the absorption baseline and broadening of the main absorption band.

The formation of heterometallic arrays by interaction of the gold complexes with Zn^{2+} and Cu^{+} salts was studied. Heterometallic complexes with a 1:1 stoichiometry were obtained, as verified by NMR, absorption and emission spectroscopy and mass spectrometry.

Spectroscopic analysis for the systems involving **1-3** and Zn(II) or Cu(I) salts (emission, NMR and IR) evidenced different coordination modes/sites for the second metal. The results indicate that Zn(II) coordinates with the nitrogen atoms of the TPA moiety whereas Cu(I) is more prone to coordinate to the alkynyl groups although additional interactions with the nitrogen atoms cannot be excluded. The resulting emission wavelength was also tuned being red-shifted in the order Au < Au/Zn < Au/Cu-Cl < Au/Cu-BF_4. DFT calculations predict intermetallic distances in the contrary order, which is in agreement with red-shift emission when metal atoms become close to each other (metallophilic contacts).

View Article Online
DOI: 10.1039/D0DT02564J

Experimental Section

General procedures

All manipulations have been performed under prepurified N_2 using standard Schlenk techniques. All solvents have been distilled from appropriated drying agents. Commercial reagents 1,3,5-triaza-7-phosphatricyclo[3.3.1.13.7]decane (PTA, Aldrich 97%), 3,7-diacetyl-1,3,7-triaza-5- phosphabicyclo[3.3.1]nonane (DAPTA, Aldrich 97%), copper (I) chloride (Aldrich, 99%), zinc nitrate hexahydrate (Aldrich, 98%). Literature methods have been used to prepare [AuCl(PR_3)] (PR_3 = PTA,[45] DAPTA,[46] PPh_3[47]), [Au(PPh_3)(acac)],[48] tetrakis(acetonitrile)copper(I) tetrafluoroborate.[49]

Physical measurements

Infrared spectra have been recorded on a FT-IR 520 Nicolet Spectrophotometer. ^{1}H NMR (δ(TMS) = 0.0 ppm), ^{31}P{^{1}H} NMR (δ(85% H_3PO_4) = 0.0 ppm) spectra have been obtained on a Varian Mercury 400 and Bruker 400 (Universitat de Barcelona). ElectroSpray-Mass spectra (+) has been recorded on a Fisons VG Quatro spectrometer (Universitat de Barcelona). High-resolution Mass have been recordered on a Waters Xevo G2-XS QTof Analyzer (University of Padova). MALDI-TOF spectra (+) has been recorded on an Applied Biosystems 4700 Proteomics Analyzer. Absorption spectra have been recorded on a Varian Cary 100 Bio UV- spectrophotometer and emission spectra on a Horiba-Jobin-Ybon SPEX Nanolog spectrofluorimeter (Universitat de Barcelona). Microanalyses were carried out at the Centres Científics i Tecnològics (Universitat de Barcelona).

Spectroscopic absorption and emission titrations

Absorption titrations. 3 mL of a neutral $1\cdot10^{-5}$ M acetonitrile solution of the corresponding gold(I) compound was introduced into a 1 cm path absorption cuvette. The titrations were carried out by addition of aliquots of $1\cdot10^{-3}$ or $1\cdot10^{-4}$ M solutions of the Zn(II) or Cu(I) salts and the corresponding absorption spectra was recorded in each point. Each titration was repeated 3 times in order to check the correct reproducibility and at 25ºC.

Emission titrations. 3 mL of a neutral $1\cdot10^{-5}$ M acetonitrile solution of the corresponding gold(I) compound was introduced into a 1 cm path emission cuvette. The titrations were carried out by addition of aliquots of $1\cdot10^{-3}$ or $1\cdot10^{-4}$ M solutions of the Zn(II) or Cu(I)

salts and the corresponding absorption spectra was recorded in each point. Each titration was repeated 3 times in order to check the correct reproducibility and at 25ºC.

Synthesis and Characterization

Synthesis of tris((6-bromopyridin-2-yl)methyl)amine (L1)

In a 250 mL double neck flask, anhydrous NH_4OAc (1.38 g, 17.9 mmol) and 6-bromo-2-pyridinecarboxaldehyde (10.00 g, 53.7 mmol) were dissolved in dry CH_2Cl_2 (170 mL) under N_2 and left under stirring for 1 hour. Three aliquots of $NaBH(OAc)_3$ (3.80 g, 17.9 mmol) were added waiting one hour between each addition. After that the reaction was stirred for 12 hours at room temperature. The solvent was removed under reduced pressure. The resulting white solid was dissolved in ethyl acetate and the solution extracted with 0.1 M solution of KOH (3x100 mL). The organic phases were dried on Na_2SO_4 and the solvent was removed under reduced pressure. The resulting solid was precipitated by crystallization from THF/hexane, yielding a white solid. Yield: 61%. m. p.: 80-84 °C. FT-IR (KBr) ν(cm^{-1}) 1131, 1403, 1444, 1554, 1581. ^{1}H NMR (200 MHz, $CDCl_3$) δ 7.63 (1H, *m*), 7.44 (1H, *d*, J = 7.4 Hz), 4.16 (1H, s). ^{13}C NMR (72.5 MHz, $CDCl_3$) δ 160.50, 141.34, 138.36, 126.38, 121.71, 59.35. ESI-MS (+) *m/z*: 527.0 ($M+H^+$, calc: 526.9). HR-ESI-MS (*) ($C_{18}H_{15}Br_3N_4 + H^+$) *m/z*= 524.8911, calc. 524.8920.

Synthesis of 2,2',2''-(((nitrolotris(methylene))tris(pyridine-6,2-diyl))tris(ethyne-2,1-diyl))tris(propan-2-ol) (L2)

Triethylamine (5.29 mL, 37,95 mmol) and 2-methyl-3-butyn-2-ol (2.20 mL, 22.77 mmol) were added to a suspension of tris((6-bromopyridin-2-yl)methyl)amine (2.00 g, 3.79 mmol) in THF dry in a Schlenk flask. After heating the mixture to 60 °C, $Pd(PPh_3)_4$ (1%, 43.83 mg, 0.04 mmol) and then CuI (2%, 14.45 mg, 0.08 mmol) were added. The reaction was stirred at 60 °C for 12 hours and without cooling down, it was filtered through Celite. The filtrate solution was dried under vacuum to gain a yellow solid. The product was purified by precipitation in THF/hexane to yield a white solid. Yield: 87%. m.p.: 80-82 °C. FT-IR (KBr) ν(cm^{-1}) 3285, 2981, 2931, 2837, 1584, 1567, 1450, 1413, 1376, 1361, 1295, 1164. ^{1}H NMR (200 MHz, $CDCl_3$) δ 7.60 (1H, *t*, J = 7.7 Hz), 7.44 (1H, *d*, J = 7.7 Hz), 7.26 (1H, *d*, J = 7.7 Hz), 3.91 (2H, *s*), 1.65 (6H, *s*). ^{13}C NMR (50 MHz, $CDCl_3$) δ 159.42, 142,46, 136.85, 125.83, 122.38, 94.23, 81.76, 65.54, 60.25, 31.25. ESI-MS (+)

View Article Online
DOI: 10.1039/D0DT02564J

m/z: 537.3 ([M + H^+], calc: 537.6). HR-ESI-MS (+) ($C_{33}H_{36}N_4O_3$ +H^+) *m/z*= 537.2874, calc. 537.2869.

Synthesis of tris((6-ethylpyridin-2-yl)methyl)amine (L)

2,2',2''-(((nitrolotris(methylene))tris(pyridine-6,2-diyl))tris(ethyne-2,1-diyl))tris(propan-2-ol) (100 mg, 0.19 mmol)was dissolved in toluene dry in a Schlenk under nitrogen atmosphere. After adding NaOH (33.57 mg, 0.84 mmol), the mixture was stirred at reflux for 1.5 hours. It was then cooled down and dried under vacuum. The light brown solid was dissolved in water and acidified with HCl 1M aqueous solution till pH 7.00. The mixture was extracted with dichloromethane and the organic phase was washed with brine. The organic phases were dried on Na_2SO_4 and the solvent was removed under reduced pressure. The product was precipitate from THF/hexane, gaining a yellowish solid. Yield: 60%. m. p.: 100-102 °C. FT-IR (KBr) ν(cm^{-1}) 3278, 3058, 2830, 1581, 1570, 1454, 1119. ^{1}H NMR (200 MHz, $CDCl_3$) δ 7.65 (2H, *m*), 7.39 (1H, *d*, J = 8.7 Hz), 3.95 (2H, *s*), 3.18 (1H, *s*). ^{13}C NMR (50 MHz, $CDCl_3$) δ 160.04, 141.76, 136.86, 126.16, 123.14, 83.07, 77.28, 60.15. ESI-MS (+) *m/z*: 363.2 ([M + H^+], calc: 363.1). HR-ESI-MS (+) ($C_{24}H_{18}N_4$ +Na^+) *m/z*= 385.1437, calc. 385.1424.

Synthesis $Au_3(PTA)_3L$ (1)

KOH (22 mg, 0.39 mmol) was added to a solution of tris((6-ethynylpyridine-2-yl)methyl)amine (35 mg, 0.096 mmol) in methanol (15 mL). After 30 min stirring, a solution of [AuCl(PTA)] (122 mg, 0.31 mmol) in dichloromethane (15 mL) was added. After 24 hours of stirring at room temperature, the solution was concentrated to ca. 15 mL and ether was added to precipitate a yellow solid. The product was isolated by filtration and dried under vacuum. Yield 63 %. ^{31}P{^{1}H} NMR (DMSO-d_6, ppm): -52.4. ^{1}H NMR (DMSO-d_6, ppm): 4.33 (s, 18H, N-CH_2-P), 4.36 (d, J = 12.4 Hz, 9H, N-CH_2-N), 4.52 (d, J = 12.4 Hz, 9H, N-CH_2-N), 7.13 (d, J = 7.6Hz, 3H, H_{Py}), 7.38 (d, J = 7.6Hz, 3H, H_{Py}), 7.64 (t, J = 8Hz, 3H, H_{Py}). IR (KBr, cm^{-1}): ν(C≡C): 2103; ν(CH_2-P): 1450; ν(C-N): 1270. ESI-MS (+) *m/z*: 1422.2739 ([M+H]$^+$, calc: 1422.2678); 1444.2575 ([M+Na]$^+$, calc: 1422.2498). Anal. Found (calcd for $C_{42}H_{51}Au_3N_{13}P_3 \cdot 4\ CH_2Cl_2$): C 31.36 (31.37); H 3.22 (3.38); N 10.28 (10.34).

Synthesis $Au_3(DAPTA)_3L$ (2)

KOH (14 mg, 0.24 mmol) was added to a solution of tris((6-ethynylpyridine-2-yl)methyl)amine (20 mg, 0.056 mmol) in methanol (15 mL). After 30 min stirring, a solution of [AuCl(DAPTA)] (80 mg, 0.17 mmol) in dichloromethane (15 mL) was added. After 24 hours of stirring at room temperature, the solution was concentrated to ca. 15 mL and ether was added to precipitate a yellow solid. The product was isolated by filtration and dried under vacuum. Yield: 40 %. $^{31}P\{^1H\}$ NMR (DMSO-d_6, ppm): 3.0. ^1H NMR (DMSO-d_6, ppm): 1.95 (s, 18H, COMe), 3.69 (s, 3H, N-CH_2-P), 3.96 (s, 6H, N-CH_2-P), 4.08 (d, J = 13.2 Hz, 3H, N-CH_2-N), 4.24 (m, 3H, N-CH_2-P), 4.62 (d, J = 12.8 Hz, 3H, N-CH_2-N), 4.80 (m, 3H, N-CH_2-P), 4.91 (d, J = 14.4 Hz, 3H, N-CH_2-N), 5.33 (m, 3H, N-CH_2-P), 5.51 (d, J = 13.2 Hz, 3H, N-CH_2-N), 7.17 (d, J = 7.6 Hz, 3H, HPy), 7.41 (d, J = 7.6 Hz, 3H, HPy), 7.66 (t, J = 7.6 Hz, 3H, HPy). IR (KBr, cm^{-1}): ν(C≡C): 2106; ν(C=O): 1636; ν(CH2-P): 1442; ν(C-N): 1234. ESI-MS (+) *m/z*: 557.098 (($[M+3H^+ + CH_3OH]^{3+}$, calc: 557.457). Anal. Found (calcd for $C_{51}H_{63}Au_3N_{13}O_6P_3 \cdot 5CH_2Cl_2$): C 32.23 (32.61); H 3.45 (3.57); N 8.93 (8.83).

Synthesis $Au_3(PPh_3)_3L$ (3)

A dichloromethane solution (4 mL) of [Au(acac)PPh_3] (55 mg, 0.10 mmol) was added dropwise to a dichloromethane solution (6 mL) of tris((6-ethynylpyridine-2-yl)methyl)amine (19 mg, 0.03 mmol). After 2 h of stirring at room temperature, the solution was concentrated under vacuum to a final volume of 3 ml and hexane was slowly added. During all the manipulations, the solution was protected from the light in order to avoid decomposition. The white suspension was separated from brown solid and it was dried under vacuum to give a yellow solid. Yield: 60%. $^{31}P\{^1H\}$ NMR ($CDCl_3$, ppm): 29.1. ^1H NMR ($CDCl_3$, ppm): 7.67 (9H, dd, *J* = 12.0, 7.6 Hz,), 7.49 (45H, m), 3.83 (6H, s). IR (KBr, cm^{-1}): ν(C≡C): 2112. ESI-MS (+) *m/z*: 1737.300 ($[M+H]^+$, calc: 1737.310). Anal. Found (calcd for $C_{78}H_{60}Au_3N_4P_3 \cdot 3\ CH_2Cl_2$): C 48.28 (48.84); H 3.06 (3.34); N 2.60 (2.81).

Synthesis of Au_3(triphos)L (4)

KOH (46 mg, 0.82 mmol) was added to a solution of tris((6-ethynylpyridine-2-yl)methyl)amine (76 mg, 0.21 mmol) in methanol (20 mL). After 30 min stirring, a solution of [$(AuCl)_3$(triphos)] (278 mg, 0.21 mmol) in dichloromethane (20 mL) was added. After 5 hours of stirring at room temperature, the solution was concentrated to ca.

20 mL and hexane was added to precipitate an orange solid. The product was isolated by filtration and dried under vacuum. Yield: 54 %. $^{31}P\{^1H\}$ NMR ($CDCl_3$, ppm): 16.9. ^1H NMR ($CDCl_3$, ppm): 0.88 (s, 3H, CH_3-C-), 3.37 (d, J = 11.6 Hz, 6H, C-CH_2-P), 7.48 (m, 18H, P-Ph), 7.79 (m, 12H, P-Ph). IR (KBr, cm^{-1}): ν(C≡C): 2113; ν(PPh_2): 1435, 1098. ESI-MS (+) *m/z*: 1592.29 ($[M+NH_4]^+$, calc: 1592.289). Anal. Found (calcd for $C_{65}H_{54}Au_3N_4P_3 \cdot 5\ CH_2Cl_2$): C 41.84 (42.05); H 3.24 (3.23); N 2.69 (2.80).

Synthesis of $[Au_3(PTA)_3LZn](NO_3)_2$ (1a)

Solid $Zn(NO_3)_2$ (2.8 mg, 9.42 x 10^{-3} mmol) was added to a solution of **1** (5 mg, 3.51 x 10^{-3} mmol) in MeOH (10 mL). The solution was stirred during 2h at room temperature and then evaporated to dryness under vacuum to yield an orange solid that was washed with methanol. Yield: 65%. $^{31}P\{^1H\}$ NMR (DMSO-d_6 ppm): -52.2. ^1H NMR (DMSO d_6 ppm): 4.33 (s, 18H, N-CH_2-P), 4.36 (d, J = 12.4 Hz, 9H, N-CH_2-N), 4.52 (d, J = 12.4 Hz, 9H, N-CH_2-N), 7.13 (d, J = 7.6 Hz, 3H, H_{Py}), 7.38 (d, J = 7.6 Hz, 3H, H_{Py}), 7.64 (t, J = 8 Hz, 3H, H_{Py}). IR (KBr, cm^{-1}): ν(C≡C): 2104; ν(CH_2-P): 1450; ν(NO^{3-}): 1383; ν(C-N): 1270. MALDI-TOF *m/z*: 1565.1 ($[[M + H_2O]+NO_3]^+$, calc.: 1565.1). Anal. Found (calcd for $C_{42}H_{51}Au_3N_{15}O_6P_3Zn \cdot 5H_2O$): C 30.05 (29.65); H 3.16 (3.61); N 12.35 (12.35).

Synthesis of $[Au_3(PTA)_3LCuCl]$ (1b)

Solid CuCl (0.51 mg, 0.005 mmol) was added to a solution of **1** (5 mg, 0.004 mmol) in CH_3CN (10 mL). The solution was stirred during 2h at room temperature and then evaporated to dryness under vacuum to yield an orange solid that was washed with acetonitrile. Yield: 80%. $^{31}P\{^1H\}$ NMR (DMSO-d_6 ppm): -52.2. ^1H NMR (DMSO-d_6 ppm): 4.33 (s, 18H, N-CH_2-P), 4.36 (d, J = 12.4 Hz, 9H, N-CH_2-N), 4.52 (d, J = 12.4 Hz, 9H, N-CH_2-N), 7.44 (d, J = 8 Hz, 3H, H_{Py}), 7.67 (d, J = 8 Hz, 3H, H_{Py}), 7.90 (t, J = 7.6 Hz, 3H, H_{Py}). IR (KBr, cm^{-1}): ν(C≡C): 2104, 2055; ν(CH_2-P): 1450; ν(C-N): 1270. MALDI-TOF *m/z*: 1561.1 ($[[M + H]+CH_3CN]^+$, calc.: 1561.1). Anal. Found (calcd for $C_{42}H_{51}Au_3ClCuN_{13}P_3 \cdot 4\ CH_2Cl_2$): C 29.47 (29.70); H 2.97 (3.20); N 9.56 (9.79).

Synthesis of $[Au_3(PTA)_3LCu]BF_4$ (1c)

Similar procedure was used in the synthesis of **1c** with respect to **1b** but using $[Cu(NCMe)_4]BF_4$ instead of CuCl. (Yield: 75%) $^{31}P\{^1H\}$ NMR (DMSO-d_6 ppm): -52.2. ^1H NMR (DMSO-d_6 ppm): 4.33 (s, 18H, N-CH_2-P), 4.36 (d, J = 12.4 Hz, 9H, N-CH_2-N), 4.52 (d, J = 12.4 Hz, 9H, N-CH_2-N), 7.44 (d, J = 8 Hz, 3H, H_{Py}), 7.67 (d, J = 8 Hz, 3H,

H_{Py}), 7.90 (t, J = 7.6 Hz, 3H, H_{Py}). IR (KBr, cm^{-1}): ν(C≡C): 2099, 2059; ν(CH_2-P): 1450; ν(C-N): 1270. MALDI-TOF *m/z*: 1592.9 ([M + DMSO]$^+$, calc.: 1562.2). Anal. Found (calcd for $C_{42}H_{51}Au_3BCuF_4N_{13}P_3 \cdot 3\ CH_2Cl_2$): C 29.88 (29.59); H 3.10 (3.14); N 9.60 (9.90).

Synthesis of $[Au_3(DAPTA)_3LZn](NO_3)_2$ (2a)

Solid $Zn(NO_3)_2 \cdot 6H_2O$ (1.3 mg, 4.37 x 10^{-3} mmol) was added to a solution of **2** (4 mg, 2.44 x 10^{-3} mmol) in MeOH (10 mL). The solution was stirred during 2h at room temperature and then evaporated to dryness under vacuum to yield a yellow solid that was washed with methanol. Yield: 55%. $^{31}P\{^1H\}$ NMR (DMSO-d_6 ppm): 3.01. ^1H NMR (DMSO-d_6 ppm): 1.95 (s, 18H, COMe), 3.70 (d, J = 15.6 Hz, 3H, N-CH_2-P), 3.99 (s, 6H, N-CH_2-P), 4.10 (d, J = 14 Hz, 3H, N-CH_2-N), 4.27 (s, 3H, N-CH_2-P), 4.61 (d, J = 13.2 Hz, 3H, N-CH_2-N), 4.79 (m, 3H, N-CH_2-P), 4.91 (d, J = 14 Hz, 3H, N-CH_2-N), 5.36 (d, J = 13.6 Hz, 3H, N-CH_2-P), 5.51 (d, J = 14 Hz, 3H, N-CH_2-N), 7.28 (d, J = 8 Hz, 3H, H_{Py}), 7.40 (d, J = 7.6 Hz, 3H, H_{Py}), 7.73 (t, J = 7.6 Hz, 3H, H_{Py}). IR (KBr, cm^{-1}): ν(C≡C): 2103; ν(C=O): 1636; ν(CH_2-P): 1440; ν(NO^{3-})1383; ν(C-N): 1232. MALDI-TOF *m/z*: 926.2 ([M + CH_2Cl_2 + $2H_2O$ + CH_3OH]$^{2+}$, calc.: 926.6). Anal. Found (calcd for $C_{51}H_{63}Au_3N_{15}O_{12}P_3Zn \cdot 5\ H_2O$): C 31.57 (31.95); H 4.01 (3.84); N 10.62 (10.96).

Synthesis of $[Au_3(DAPTA)_3LCuCl]$ (2b)

Solid CuCl (0.43 mg, 4.34 x 10^{-3} mmol) was added to a solution of **2** (5.3 mg, 3.24 x 10^{-3} mmol) in CH3CN (10 mL). The solution was stirred for 2h at room temperature and then evaporated to dryness under vacuum to yield an orange solid that was washed with acetonitrile. Yield: 85%. $^{31}P\{^1H\}$ NMR (DMSO-d_6 ppm): 3.01. ^1H NMR (DMSO-d_6 ppm): 1.97 (s, 18H, COMe), 3.71 (d, J = 14 Hz, 3H, N-CH_2-P), 3.97 (s, 6H, N-CH_2-P), 4.10 (d, J = 13.6 Hz, 3H, N-CH_2-N), 4.24 (d, J = 12.4 Hz, 3H, N.CH_2-P), 4.34 (s, 6H, N-CH_2-Py), 4.62 (d, J = 13.6 Hz, 3H, N-CH_2-N), 4.81 (m, 3H, N-CH_2-P), 4.92 (d, J = 14 Hz, 3H, N-CH_2-N), 5.34 (m, 3H, N-CH_2-P), 5.52 (d, J = 13.2 Hz, 3H, N-CH_2-N), 7.44 (d, J = 7.6 Hz, 3H, H_{Py}), 7.67 (d, J = 7.2 Hz, 3H, H_{Py}), 7.90 (t, J = 7.6 Hz 3H, H_{Py}). IR (KBr, cm^{-1}): ν(C≡C): 2103, 2060; ν(C=O): 1628; ν(CH_2-P): 1444; ν(C-N): 1232. MALDI-TOF *m/z*: 1790.9 ([M + H + $3H_2O$]$^+$, calc.: 1790.3). Anal. Found (calcd for $C_{51}H_{63}Au_3ClCuN_{13}O_6P_3 \cdot 3\ CH_2Cl_2 \cdot 2\ H_2O$): C 31.65 (31.99); H 3.47 (3.63); N 8.65 (8.98).

Synthesis of $[Au_3(DAPTA)_3LCu][BF_4]$ (2c)

View Article Online
DOI: 10.1039/D0DT02564J

Similar procedure was used in the synthesis of **2c** with respect to **2b** but using $[Cu(NCMe)_4]BF_4$ instead of CuCl. Yield: 74%. $^{31}P\{^1H\}$ NMR (DMSO-d_6 ppm): 3.01. ^1H NMR (DMSO-d_6 ppm): 1.97 (s, 18H, COMe), 3.70 (d, J = 15.2 Hz, 3H, N-CH_2-P), 3.96 (s, 6H, N-CH_2-P), 4.10 (d, J = 14 Hz, 3H, N-CH_2-N), 4.24 (d, J = 14 Hz, 3H, N-CH_2-P), 4.34 (s, 6H, N-CH_2-Py), 4.62 (d, J = 14 Hz, 3H, N-CH_2-N), 4.79 (m, 3H, N-CH_2-P), 4.92 (d, J = 13.6 Hz, 3H, N-CH_2-N), 5.33 (m, 3H, N-CH_2-P), 5.53 (d, J = 13.2 Hz, 3H, N-CH_2-N), 7.44 (d, J = 7.6 Hz, 3H, H_{Py}), 7.67 (d, J = 7.6 Hz, 3H, H_{Py}), 7.90 (t, J = 7.6 Hz, 3H, H_{Py}). IR (KBr, cm^{-1}): ν(C≡C): 2098, 2055; ν(C=O): 1637; ν(CH_2-P): 1439; ν(C-N): 1232. Anal. Found (calcd for $C_{51}H_{63}Au_3BCuF_4N_{13}O_6P_3 \cdot 2CH_2Cl_2 \cdot H_2O$): C 32.02 (32.21); H 3.26 (3.52); N 9.12 (9.21).

Synthesis of $[Au_3(PPh_3)_3LZn](NO_3)_2$ (3a)

Solid $Zn(NO_3)_2 \cdot 6H_2O$ (1.71 mg, 5.76 x 10^{-3} mmol) was added to a solution of **3** (5.0 mg, 2.88 x 10^{-3} mmol) in MeOH (10 mL). The solution was stirred during 2h at room temperature and then evaporated to dryness under vacuum to yield a yellow solid that was washed with methanol. Yield: 55%. $^{31}P\{^1H\}$ NMR (CD_3CN ppm): 33.0. ^1H NMR (CD_3CN ppm): 3.75 (s, 6H, CH_2), 7.42 (d, J = 8Hz, 3H, Py), 7.62 (m, 45H, PPh_3), 7.78 (d, J = 8 Hz, 3H, Py), 7.94 (t, J = 8 Hz, 3H, Py). IR (KBr, cm^{-1}): ν(C≡C): 2103; ν(C=O): 1636; ν(CH_2-P): 1440; ν(NO^{3-})1383; ν(C-N): 1232. Anal. Found (calcd for $C_{78}H_{60}Au_3N_6O_6P_3Zn \cdot 5\,H_2O$): C 46.70 (46.46); H 3.75 (3.50); N 4.25 (4.17).

Synthesis of $[Au_3(PPh_3)_3LCuCl]$ (3b)

Solid CuCl (0.34 mg, 3.45 x 10^{-3} mmol) was added to a solution of **3** (6 mg, 3.45 x 10^{-3} mmol) in CH_3CN (10 mL). The solution was stirred during 2h at room temperature and then evaporated to dryness under vacuum to yield an orange solid that was washed with acetonitrile. Yield: 50%. $^{31}P\{^1H\}$ NMR (CD_3CN ppm): 33.0. ^1H NMR (CD_3CN ppm): 3.27 (s, 6H, CH_2), 7.29 (d, J = 7.6 Hz, 3H, Py), 7.49 (m, 45H, PPh_3), 7.64 (d, J = 6.8 Hz, 3H, Py), 7.76 (t, J = 8 Hz, 3H, Py). IR (KBr, cm^{-1}): ν(C≡C): 2100, 2080; ν(CH_2-P): 1453; ν(C-N): 1265. Anal. Found (calcd for $C_{78}H_{60}Au_3CuClN_4P_3 \cdot 3\,CH_2Cl_2$): C 46.73 (46.53); H 3.33 (3.18); N 2.86 (2.68).

Synthesis of $[Au_3(PPh_3)_3LCu]BF_4$ (3c)

Similar procedure was used in the synthesis of **3c** with respect to **3b** but using $[Cu(NCMe)_4]BF_4$ instead of CuCl. Yield: 75%. $^{31}P\{^1H\}$ NMR (CD_3CN ppm): 33.0. ^1H

NMR (CD_3CN ppm): 4.23 (s, 6H, CH_2), 7.30 (d, J = 7.6 Hz, 3H, Py), 7.39 (d, J = 7.6 Hz, 3H, Py), 7.52 (m, 45H, PPh_3), 7.74 (t, J = 7.6 Hz, 3H, Py). IR (KBr, cm^{-1}): ν(C≡C): 2099, 2059; ν(CH_2-P): 1450; ν(C-N): 1270. Anal. Found (calcd for $C_{78}H_{60}Au_3CuBF_4N_4P_3 \cdot 4\ CH_2Cl_2$): C 44.34 (44.22); H 3.45 (3.08); N 2.7 (2.52).

Synthesis of $[Au_3(triphos)LZn](NO_3)_2$ (4a)

KOH (16.1 mg, 0.3 mmol) was added to a solution of tris((6-ethynylpyridine-2-yl)methyl)amine (20 mg, 0.055 mmol) in methanol (15 mL). After 30 min stirring a solution of $(AuCl)_3$(triphos) (75 mg, 0.057 mmol) and $Zn(NO_3)_2 \cdot 6H_2O$ (33 mg, 0.11 mmol) in a mixture of methanol/dichloromethane (1:2) (15 mL) was added. After 5 hours of stirring at room temperature the solution was concentrated to ca. 15 mL and hexane was added to precipitate an orange solid. The product was isolated by filtration and dried under vacuum. Yield 85%. $^{31}P\{^1H\}$ NMR (DMSO-d_6, ppm): 17.4. ^1H NMR (DMSO-d_6, ppm): 7.1-7.9 (m, 3H, P-Ph). IR (KBr, cm^{-1}): ν(C≡C): 2108; ν(PPh_2): 1432, 1094**.** MALDI-TOF *m/z*: 819.0 (M^{2+}, calc.: 819.0). Anal. Found (calcd for $C_{65}H_{54}Au_3N_6O_6P_3Zn \cdot 5\ H_2O$): C 41.85 (42.10); H 3.26 (3.48); N 4.32 (4.53).

Synthesis of $[Au_3(triphos)LCuCl]$ (4b)

KOH (11.1 mg, 0.2 mmol) was added to a solution of tris((6-ethynylpyridine-2-yl)methyl)amine (19.5 mg, 0.054 mmol) in methanol (15 mL). After 30 min stirring, a solution of $(AuCl)_3$(triphos) (73.6 mg, 0.056 mmol) and CuCl (5.9 mg, 0.059 mmol) in a mixture of acetonitrile/dichloromethane (1:2) (15 mL) was added. After 5 hours of stirring at room temperature the solution was concentrated to ca. 15 mL and hexane was added to precipitate an orange solid. The product was isolated by filtration and dried under vacuum. Yield 75 %. $^{31}P\{^1H\}$ NMR (DMSO-d_6, ppm): 17.4. ^1H NMR (DMSO-d_6, ppm): 7.1-7.9 (m, 3H, P-Ph). IR (KBr, cm^{-1}): ν(C≡C): 2108, 1957; ν(PPh_2): 1432, 1098. MALDI-TOF *m/z*: 1673.1 ($[M + H]^+$, calc.: 1673.1). Anal. Found (calcd for $C_{65}H_{54}Au_3CuClN_4P_3 \cdot 3\ CH_2Cl_2 \cdot 2\ H_2O$): C 41.75 (41.57); H 3.26 (3.28); N 2.69 (2.85).

Synthesis of $[Au_3(triphos)LCu]BF_4$ (4c)

Similar procedure was used in the synthesis of **4c** with respect to **4b** but using $[Cu(NCMe)_4]BF_4$ instead of CuCl. Yield 80 %. $^{31}P\{^1H\}$ NMR (DMSO-d_6, ppm): 17.4. ^1H NMR (DMSO-d_6, ppm): 7.1-7.9 (m, 3H, P-Ph). IR (KBr, cm^{-1}): ν(C≡C): 2113, 1957;

View Article Online
DOI: 10.1039/D0DT02564J

ν(PPh_2): 1436, 1098. MALDI-TOF *m/z*: 1637.0 (M^+, calc.: 1637.2). Anal. Found (calcd for $C_{65}H_{54}Au_3CuBF_4N_4P_3 \cdot 2\ CH_2Cl_2$): C 42.1 (42.46); H 3.36 (3.08); N 3.1 (2.96).

Computational details

All compounds were minimised with the Gaussian16 program package.[50] at the DFT level of theory with a hybrid density functional PBE0.[51] The basis set consisted of a quasi-relativistic effective core potential basis set def2-TZVPPD for gold atoms and 6-31G(d,p) for all atoms.[52] Frequencies were calculated to verify the minima.

Acknowledgements

Authors are grateful to the Ministerio de Ciencia e Innovación of Spain (AEI/FEDER, UE Projects CTQ2016-76120-P and 2019-104121GB-I00). G.S. is indebted for a fellowship from MIUR (Progetto Competitivo CMPT148505). A.P. is indebted to an FI predoctoral fellowship from the Generalitat de Catalunya. The project has been carried out in the frame of COST Actions CM1402 Crystallize (G.S. STSM). This research was supported by a Marie Curie Intra-European Fellowship within the 7th European Community Framework Programme (R. G.).

Supporting Information

NMR spectra of TPA ligand and homometallic and heterometallic complexes. Absorption and emission spectra of the compounds in solution and in solid state. Absorption and emission titrations of the gold complexes with Zn(II) and Cu(I) salts. Schemes for the synthesis of the complexes. XYZ coordinates of computed species **1** and **1a-c**.

References

1 J. Liang, J. Zhang, L. Zhu, A. Duarandin, V. G. Young, N. Geacintov and J. W. Canary, *Inorg. Chem.*, 2009, **48**, 11196–11208.

2 F. Weisser, H. Stevens, J. Klein, M. van der Meer, S. Hohloch and B. Sarkar, *Chem. - A Eur. J.*, 2015, **21**, 8926–8938.

3 F. A. Scaramuzzo, E. Badetti, G. Licini and C. Zonta, *Chirality*, 2019, **31**, 375–383.

4 C. Bravin, E. Badetti, R. Puttreddy, F. Pan, K. Rissanen, G. Licini and C. Zonta, *Chem. - A Eur. J.*, 2018, **24**, 2936–2943.

5 C. Bravin, A. Guidetti, G. Licini and C. Zonta, *Chem. Sci.*, 2019, **10**, 3523–3528.

6 C. Bravin, G. Licini, C. A. Hunter and C. Zonta, *Chem. Sci.*, 2019, **10**, 1466–1471.

7 N. A. Carmo dos Santos, F. Lorandi, E. Badetti, K. Wurst, A. A. Isse, A. Gennaro, G. Licini and C. Zonta, *Polymer*, 2017, **128**, 169–176.

8 M. Natali, E. Badetti, E. Deponti, M. Gamberoni, F. A. Scaramuzzo, A. Sartorel and C. Zonta, *Dalton Trans.*, 2016, **45**, 14764–14773.

9 J. C. Lima and L. Rodríguez, *Chem. Soc. Rev.*, 2011, **40**, 5442-5456.

10 E. Aguiló, A. J. Moro, M. Outis, J. Pina, D. Sarmento, J. S. Seixas de Melo, L. Rodríguez and J. C. Lima, *Inorg. Chem.*, 2018, **57**, 13423–13430.

11 V. W.-W. Yam and E. C.-C. Cheng, *Chem. Soc. Rev.*, 2008, **37**, 1806-1813.

12 J. R. Shakirova, E. V. Grachova, V. V. Gurzhiy, S. K. Thangaraj, J. Jänis, A. S. Melnikov, A. J. Karttunen, S. P. Tunik and I. O. Koshevoy, *Angew. Chemie Int. Ed.*, 2018, **57**, 14154–14158.

13 E. V. Peris and S. Ibáñez, *Chem. – A Eur. J.*, 2019, 1–6.

14 N. Svahn, A. J. Moro, C. Roma-Rodrigues, R. Puttreddy, K. Rissanen, P. V. Baptista, A. R. Fernandes, J. C. Lima and L. Rodríguez, *Chem. - A Eur. J.*, 2018, **24**, 14654–14667.

15 A. Pinto, N. Svahn, J. C. Lima and L. Rodríguez, *Dalton Trans.*, 2017, **46**, 11125–11139.

16 E. Aguiló, A. J. Moro, R. Gavara, I. Alfonso, Y. Pérez, F. Zaccaria, C. F. Guerra, M. Malfois, C. Baucells, M. Ferrer, J. C. Lima and L. Rodríguez, *Inorg. Chem.*, 2018, **57**, 1017–1028.

17 (a) A. Pinto, G. Hernández, R. Gavara, E. Aguiló, A. J. Moro, G. Aullón, M. Malfois, J. C. Lima and L. Rodríguez, *New J. Chem.*, 2019, **43**, 8279–8289; (b) D.G. Goreinstein in Phosphorus-31 NMR. Principales and Applications, Chapter 1 "Phosphorus-31 Chemical Shifts: Principles and Empirical Observations", 1984, pp. 7-36. Ed. D.G. Goreinstein. Academic Press Inc.

18 M. Pujadas and L. Rodríguez, *Coord. Chem. Rev.*, 2020, **408**, 213179.

19 A. Belyaev, T. M. Dau, J. Jänis, E. V. Grachova, S. P. Tunik and I. O. Koshevoy,

View Article Online
DOI: 10.1039/D0DT02564J

Organometallics, 2016, **35**, 3763–3774.

20 F. A. Scaramuzzo, G. Licini and C. Zonta, *Chem. – A Eur. J.*, 2013, **19**, 16809–16813.

21 R. Gavara, J. Llorca, J. C. Lima and L. Rodríguez, *Chem. Commun.*, 2013, **49**, 72–74.

22 E. Aguiló, R. Gavara, C. Baucells, M. Guitart, J. C. Lima, J. Llorca and L. Rodríguez, *Dalton Trans.*, 2016, **45**, 7328–7339.

23 R. Gavara, J. C. Lima and L. Rodríguez, *Photochem. Photobiol. Sci.*, 2016, **15**, 635–643.

24 M. Ferrer, A. Gutiérrez, L. Rodríguez, O. Rossell, J. C. Lima, M. Font-Bardia and X. Solans, *Eur. J. Inorg. Chem.*, 2008, **2008**, 2899–2909.

25 L. Rodríguez, M. Ferrer, R. Crehuet, J. Anglada and J. C. Lima, *Inorg. Chem.*, 2012, **51**, 7636–7641.

26 F. K.-W. Hau, X. He, W. H. Lam and V. W.-W. Yam, *Chem. Commun.*, 2011, **47**, 8778.

27 X. He, W. H. Lam, N. Zhu and V. W.-W. Yam, *Chem. - A Eur. J.*, 2009, **15**, 8842–8851.

28 A. Chu, F. K.-W. Hau and V. W.-W. Yam, *Chem. - A Eur. J.*, 2017, **23**, 11076–11084.

29 Y. P. Zhou, E. B. Liu, J. Wang and H. Y. Chao, *Inorg. Chem.*, 2013, **52**, 8629–8637.

30 L. Rodríguez, C. Lodeiro, J. C. Lima and R. Crehuet, *Inorg. Chem.*, 2008, **47**, 4952–4962.

31 J. R. Shakirova, E. V. Grachova, A. S. Melnikov, V. V. Gurzhiy, S. P. Tunik, M. Haukka, T. A. Pakkanen and I. O. Koshevoy, *Organometallics*, 2013, **32**, 4061–4069.

32 B. Pedras, E. Oliveira, H. Santos, L. Rodríguez, R. Crehuet, T. Avilés, J. L. Capelo and C. Lodeiro, *Inorg. Chim. Acta*, 2009, **362**, 2627–2635.

33 Analysis performd by HypSpec software for Windows, Protonics Software http://www.hyperquad.co.uk/HypSpec.htm.

34 S. Zahn and J. W. Canary, *J. Am. Chem. Soc.*, 2002, **124**, 9204–9211.

35 J. W. Canary, S. Mortezaei and J. Liang, *Coord. Chem. Rev.*, 2010, **254**, 2249–2266.

36 I. S. Krytchankou, D. V. Krupenya, V. V. Gurzhiy, A. A. Belyaev, A. J. Karttunen, I. O. Koshevoy, A. S. Melnikov and S. P. Tunik, *J. Organomet. Chem.*, 2013, **723**, 65–71.

37 I. O. Koshevoy, A. J. Karttunen, S. P. Tunik, M. Haukka, S. I. Selivanov, A. S. Melnikov, P. Y. Serdobintsev, M. A. Khodorkovskiy and T. A. Pakkanen, *Inorg. Chem.*, 2008, **47**, 9478–9488.

38 I. O. Koshevoy, A. J. Karttunen, Y. C. Lin, C. C. Lin, P. T. Chou, S. P. Tunik, M. Haukka and T. A. Pakkanen, *Dalton Trans.*, 2010, **39**, 2395–2403.

39 I. O. Koshevoy, Y.-C. Chang, A. J. Karttunen, M. Haukka, T. Pakkanen and P. Chou, *J. Am. Chem. Soc.*, 2012, **134**, 6564–6567.

40 E. W. Ainscough, A. M. Brodie, S. L. Ingham and J. M. Waters, *Inorg. Chim. Acta*, 1996, **249**, 47–55.

41 V. Pirovano, E. Brambilla and G. Tseberlidis, *Org. Lett.*, 2018, **20**, 405–408.

42 S. Neogi, Y. Lorenz, M. Engeser, D. Samanta and M. Schmittel, *Inorg. Chem.*, 2013, **52**, 6975–6984.

43 D. V. Krupenya, P. A. Snegurov, E. V. Grachova, V. V. Gurzhiy, S. P. Tunik, A. S. Melnikov, P. Y. Serdobintsev, E. G. Vlakh, E. S. Sinitsyna and T. B. Tennikova, *Inorg. Chem.*, 2013, **52**, 12521–12528.

44 P. Y. Dereza, I. S. Krytchankou, D. V. Krupenya, V. V. Gurzhiy, I. O. Koshevoy, A. S. Melnikov and S. P. Tunik, *Z. Anorg. Allg. Chemie*, 2013, **639**, 398–402.

45 Z. Assefa, B. G. McBurnett, R. J. Staples, J. P. Fackler, B. Assmann, K. Angermaier and H. Schmidbaur, *Inorg. Chem.*, 1995, **34**, 75–83.

46 E. Vergara, S. Miranda, F. Mohr, E. Cerrada, E. R. T. Tiekink, P. Romero, A. Mendía and M. Laguna, *Eur. J. Inorg. Chem.*, 2007, 2926–2933.

47 C. Kowala and J. Swan, *Aust. J. Chem.*, 1966, **19**, 547.

48 M. T. Vicente, J.; Chicote, *Inorg. Synth.*, 1998, **32**, 172.

49 G. J. Kubas, B. Monzyk and A. L. Crumbliss, in *Inorg. Synth.*, Chpater 3 " Transition Metal Compounds and Complexes**"** 2007, **19**, 90–92. Ed. Duward F. Shriver

50 M. J. Frisch, G. W. Trucks, H. B. Schlegel, G. E. Scuseria, M. A. Robb, J. R. Cheeseman, G. Scalmani, V. Barone, G. A. Petersson, H. Nakatsuji, X. Li, M. Caricato, A. V. Marenich, J. Bloino, B. G. Janesko, R. Gomperts, B. Mennucci, H. P. Hratchian, J. V. Ortiz, A. F. Izmaylov, J. L. Sonnenberg, D. Williams-Young, F. Ding, F. Lipparini, F. Egidi, J. Goings, B. Peng, A. Petrone, T. Henderson, D. Ranasinghe, V. G. Zakrzewski, J. Gao, N. Rega, G. Zheng, W. Liang, M. Hada, M. Ehara, K. Toyota, R. Fukuda, J. Hasegawa, M. Ishida, T. Nakajima, Y. Honda, O. Kitao, H. Nakai, T. Vreven, K. Throssell, J. A. Montgomery, Jr., J. E. Peralta, F. Ogliaro, M. J. Bearpark, J. J. Heyd, E. N. Brothers, K. N. Kudin, V. N. Staroverov, T. A. Keith, R. Kobayashi, J. Normand, K. Raghavachari, A. P. Rendell, J. C. Burant, S. S. Iyengar, J. Tomasi, M. Cossi, J. M. Millam, M. Klene, C. Adamo, R. Cammi, J. W. Ochterski, R. L. Martin, K. Morokuma, O. Farkas, J. B. Foresman, and D. J. Fox, Gaussian, Inc., Wallingford CT, **2016**.

51 J. P. Perdew, K. Burke and M. Ernzerhof, *Phys. Rev. Lett.*, 1996, **77**, 3865–3868.

52 A. N. Chernyshev, M. V. Chernysheva, P. Hirva, V. Y. Kukushkin and M. Haukka, *Dalton Trans.*, 2015, **44**, 14523–14531.

View Article Online
DOI: 10.1039/D0DT02564J

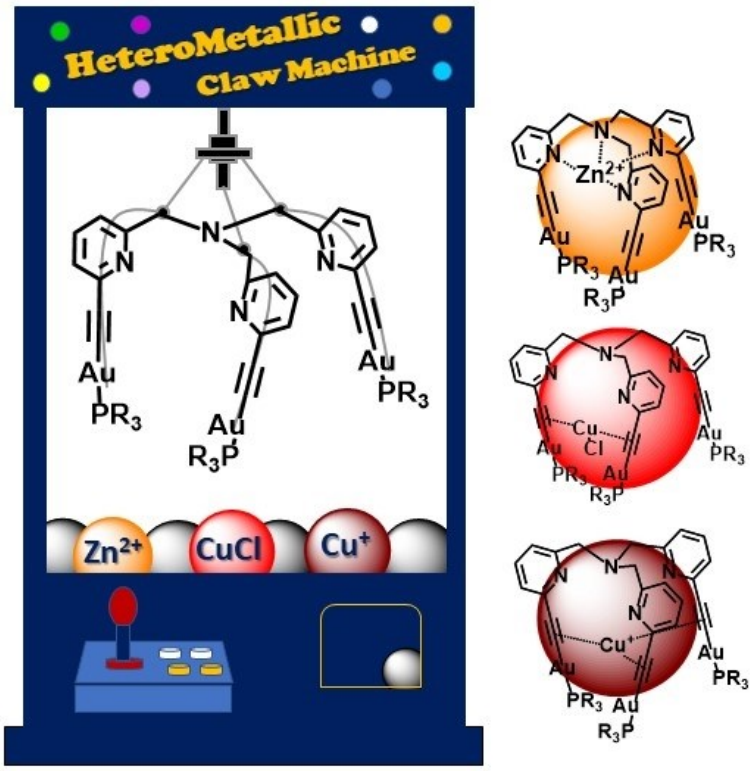

179x194mm (96 x 96 DPI)